Spectrochimica Acta Part A: Molecular and Biomolecular Spectroscopy 114 (2013) 27–32

Contents lists available at SciVerse ScienceDirect

Spectrochimica Acta Part A: Molecular and Biomolecular Spectroscopy

journal homepage: www.elsevier.com/locate/saa

Vibrational spectroscopy of the mineral meyerhofferite $CaB_3O_3(OH)_5{\cdot}H_2O$ – An assessment of the molecular structure

Ray L. Frost [a,*], Andrés López [a], Yunfei Xi [a], Ricardo Scholz [b], Geraldo Magela da Costa [c] Fernanda M. Belotti [d], Rosa Malena Fernandes Lima [e]

[a] School of Chemistry, Physics and Mechanical Engineering, Science and Engineering Faculty, Queensland University of Technology, GPO Box 2434, Brisbane, Queensland 4001, Australia
[b] Geology Department, School of Mines, Federal University of Ouro Preto, Campus Morro do Cruzeiro, Ouro Preto, MG 35,400-00, Brazil
[c] Chemistry Department, Federal University of Ouro Preto, Campus Morro do Cruzeiro, Ouro Preto, MG 35,400-00, Brazil
[d] Federal University of Itajubá, Campus Itabira, Itabira, MG 35,903-087, Brazil
[e] Mining Engineering Department, School of Mines, Federal University of Ouro Preto, Campus Morro do Cruzeiro, Ouro Preto, MG 35,400-00, Brazil

HIGHLIGHTS

- Meyerhofferite $Ca_2(H_3B_3O_7)_2{\cdot}4H_2O$ is found in sedimentary or lake-bed borate deposits.
- We have studied the Raman and infrared spectra.
- We have assessed the molecular structure of meyerhofferite.
- A comparison is made between the Raman and infrared spectrum.
- Raman spectroscopy proved far more useful for the detection of meyerhofferite than infrared spectroscopy.

GRAPHICAL ABSTRACT

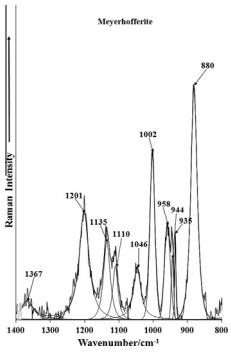

ARTICLE INFO

Article history:
Received 18 March 2013
Received in revised form 6 May 2013
Accepted 7 May 2013
Available online 20 May 2013

Keywords:
Raman spectroscopy
Borate
Meyerhofferite
Inyoite
Colemanite

ABSTRACT

Meyerhofferite is a calcium hydrated borate mineral with ideal formula: $CaB_3O_3(OH)_5{\cdot}H_2O$ and occurs as white complex acicular to crude crystals with length up to ~4 cm, in fibrous divergent, radiating aggregates or reticulated and is often found in sedimentary or lake-bed borate deposits.

The Raman spectrum of meyerhofferite is dominated by intense sharp band at 880 cm^{-1} assigned to the symmetric stretching mode of trigonal boron. Broad Raman bands at 1046, 1110, 1135 and 1201 cm^{-1} are attributed to BOH in-plane bending modes. Raman bands in the 900–1000 cm^{-1} spectral region are assigned to the antisymmetric stretching of tetrahedral boron. Distinct OH stretching Raman bands are observed at 3400, 3483 and 3608 cm^{-1}. The mineral meyerhofferite has a distinct Raman spectrum which is different from the spectrum of other borate minerals, making Raman spectroscopy a very useful tool for the detection of meyerhofferite in sedimentary and lake bed deposits.

Introduction

Meyerhofferite is a calcium hydrated borate mineral of ideal formula $CaB_3O_3(OH)_5{\cdot}H_2O$ and occurs chiefly as an alteration product of inyoite $Ca(H_4B_3O_7)(OH){\cdot}4H_2O$, another mineral [1]. The mineral was first discovered in Death Valley, USA in 1914 [2]. The mineral shows a complex acicular to crude crystals with lengths up to ~4 cm, in fibrous divergent, radiating aggregates, and is commonly reticulated [3]. The mineral shows some sort of topotactical relationship with inyoite [1]. It is often found with colemanite $Ca(B_3O_4(OH)_3){\cdot}H_2O$. The mineral is often found in sedimentary or lake-bed borate deposits [4].

* Corresponding author. Tel.: +61 7 3138 2407; fax: +61 7 3138 1804.
E-mail address: r.frost@qut.edu.au (R.L. Frost).

1386-1425/$ - see front matter © 2013 Elsevier B.V. All rights reserved.
http://dx.doi.org/10.1016/j.saa.2013.05.016

Meyerhofferite is triclinic with *Point Group:* 1 bar [5–7]. The structure was first determined by Palache [8] and latter refined by Burns and Hawthorne [9]. The cell data is *space group: P*1 with $a = 6.632(1)$ Å, $b = 8.337(1)$ Å, $c = 6.4748(6)$ Å, $\alpha = 90.81°(1)$, $\beta = 101.97°(1)$, $\gamma = 86.76°(1)$ and $Z = 2$. The hydrogen bond arrangement in the meyerhofferite has been determined [9]. Bonding between the heteropolyhedral chains is through H bonding only, with 6 H bonds along [100], 4 along [010] and 4 between elements of the same heteropolyhedral chain per unit cell. The thermal stability of the mineral has been assessed [10,11]. This research shows the decomposition temperature and mass losses.

Vibrational spectroscopy has been applied to borate glasses [12–15]. There have been a number of studies of borate glasses doped with a wide range of radioactive atoms [16,17]. Borate glasses are used as a means of containment of radioactive materials. There have been a number of studies looking at the effect of radiation on borate glasses [18,19]. If there is to be an understanding of borate glasses and their role in radioactive element containment, then an understanding of the vibrational spectroscopy of borate minerals needs to be undertaken. The number of vibrational spectroscopic studies of borate minerals is quite few and far between [20–23]. The number of Raman studies of borate minerals is also very limited [24,25]. There have been a number of infrared studies of some natural borates [26–29]. Most of these references are not new and there have been no recent studies on the vibrational spectroscopy of natural borates. Ross in Farmer's treatise reported the infrared spectra of several borate minerals [30]. The use of infrared spectroscopy is limited by the spatial resolution of the technique which is around 25 μm. In comparison, the spatial resolution using Raman spectroscopy is 1 μm. Thus, when studying a mineral using spectroscopic techniques it is advantageous to use Raman spectroscopy. The selection of the target mineral is more easily made. With infrared spectroscopy, any impurities will be measured as well as the target mineral.

Yet, there remains the issue of the vibrational spectroscopic study of natural borate minerals. In this research, our objective is to study the Raman and infrared spectra of the mineral meyerhofferite and relate the spectra to the structure of the mineral.

Experimental

Samples and preparation

Off white meyerhofferite single crystals were obtained from the collection of the Geology Department of the Federal University of Ouro Preto, Minas Gerais, Brazil, with sample code SAA-121. The mineral originated from the Bigadic deposits, Turkey [31–33]. Meyerhofferite occurs in evaporate sediments. The crystals are in association with other borates such as hydroboracite, inyoite and gypsum. The studied sample was gently crushed and the pure fragments were selected under a stereomicroscope Leica MZ4.

X-ray diffraction

X-ray diffractograms were obtained in a Shimadzu XRD 6000 diffractometer equipped with an iron tube and a graphite monochromator. The scans were done between 10–60° (2θ) with a scanning speed of 0.5°/min. Silicon was used as an internal standard. Cell parameters were refined by means of the Jade$^+$ program using least-square refinement after subtracting the background and the $K_{\alpha 2}$ contribution and using intensity and angular weighting of the most intense peaks.

Chemical characterization

Chemical study was done with support of Scanning Electron Microscopy (SEM) and Electron Microprobe (EMP). Experiments and analyses involving electron microscopy were performed in the Center of Microscopy of the Federal University of Minas Gerais, Belo Horizonte, Minas Gerais, Brazil (http://www.microscopia.ufmg.br).

Meyerhofferite crystals were coated with a 5 nm layer of evaporated carbon. Secondary Electron and Backscattering Electron images were obtained using a JEOL JSM-6360LV equipment. Qualitative and semi-quantitative chemical analyses in the EDS mode were performed with a ThermoNORAN spectrometer model Quest and was applied to support the mineral characterization and to determine potential contaminants or chemical zonation.

A quantitative chemical analysis was carried via EMP. A meyerhofferite fragment selected for this study was analyzed with the performance of four spots. The chemical analysis was carried out with a Jeol JXA8900R spectrometer from the Physics Department of the Federal University of Minas Gerais, Belo Horizonte. For each selected element was used the following standards: Fe – Magnetite, Mn – Rodhonite, Zn – Sphalerite, F – Fluorite, As – Arsenopyrite, P – $Ca_2P_2O_7$, Ca, Si and Al – Anorthite100 and Mg – MgO. The epoxy embedded meyerhofferite sample was polished in the sequence of 9 μm, 6 μm and 1 μm diamond paste MetaDI® II Diamond Paste – Buhler, using water as a lubricant, with a semi-automatic MiniMet® 1000 Grinder–Polisher – Buehler. Finally, the epoxy embedded sample was coated with a thin layer of evaporated carbon. The electron probe microanalysis in the WDS (wavelength dispersive spectrometer) mode was obtained at 15 kV accelerating voltage and beam current of 10 nA. Chemical formula was calculated on the basis of nine oxygen atoms.

Raman spectroscopy

Crystals of meyerhofferite were placed on a polished metal surface on the stage of an Olympus BHSM microscope, which is equipped with 10×, 20×, and 50× objectives. The microscope is part of a Renishaw 1000 Raman microscope system, which also includes a monochromator, a filter system and a CCD detector (1024 pixels). The Raman spectra were excited by a Spectra-Physics model 127 He–Ne laser producing highly polarized light at 633 nm and collected at a nominal resolution of 2 cm^{-1} and a precision of ±1 cm^{-1} in the range between 200 and 4000 cm^{-1}. Repeated acquisitions on the crystals using the highest magnification (50×) were accumulated to improve the signal to noise ratio of the spectra. Spectra were calibrated using the 520.5 cm^{-1} line of a silicon wafer. The Raman spectrum of at least 10 crystals was collected to ensure the consistency of the spectra.

Infrared spectroscopy

Infrared spectra were obtained using a Nicolet Nexus 870 FTIR spectrometer with a smart endurance single bounce diamond ATR cell. Spectra over the 4000–525 cm^{-1} range were obtained by the co-addition of 128 scans with a resolution of 4 cm^{-1} and a mirror velocity of 0.6329 cm/s. Spectra were co-added to improve the signal to noise ratio.

Spectral manipulation such as baseline correction/adjustment and smoothing were performed using the Spectracalc software package GRAMS (Galactic Industries Corporation, NH, USA). Band component analysis was undertaken using the Jandel 'Peakfit' software package that enabled the type of fitting function to be selected and allows specific parameters to be fixed or varied accordingly. Band fitting was done using a Lorentzian–Gaussian cross-product function with the minimum number of component bands used for the fitting process. The Gaussian–Lorentzian ratio was maintained at values greater than 0.7 and fitting was undertaken until reproducible results were obtained with squared correlations of r^2 greater than 0.995.

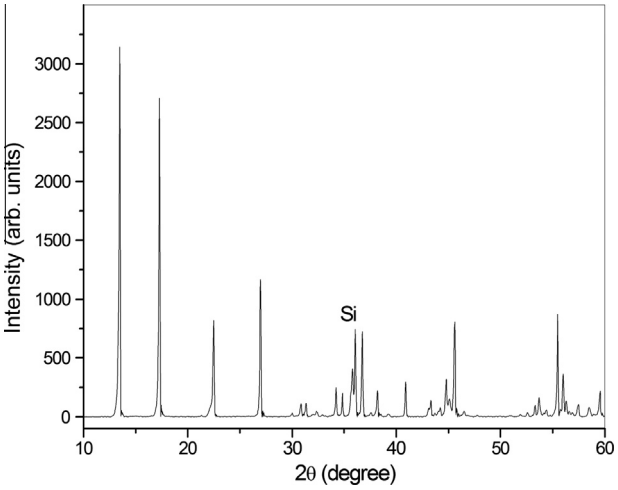

Fig. 1. X-ray diffraction pattern of meyerhofferite. Silicon was added as a internal standard.

Results and discussion

Mineral characterization

The X-ray diffraction pattern of is shown in Fig. 1. All the major peaks can be associated to meyerhofferite, but there are a few low-intensity peaks that could not be properly identified. Considering their low intensities, it is estimated that this minor phase contributes with less than 5% w/w for the total sample. The refined cell-parameters were found as: $a = 6.637(4)$, $b = 8.354(4)$, and $c = 6.477(3)$, in good agreement with the literature values (pdf file 12-0411). Other commonly associated minerals, such as gypsum, hydroboracite and inyoite were not observed.

The Backscattering Image (BSI) image of meyerhofferite sample studied in this work is shown in Fig. 2. The image shows a fragment of a single crystal, with prismatic form along the *c* axis. The image shows three perfect cleavage directions and no zonation is observed. Qualitative chemical analysis shows a homogeneous composition, with predominance of Ca (Fig. 3). In the EDS spectra, minor amounts of Al were also observed.

The thermogravimetric analysis is presented in Fig. 4. The TG curve shows a main decomposition at 217 °C followed by a second decomposition centered at about 436 °C. The total loss of mass is 27.8% upon heating up to 1000 °C.

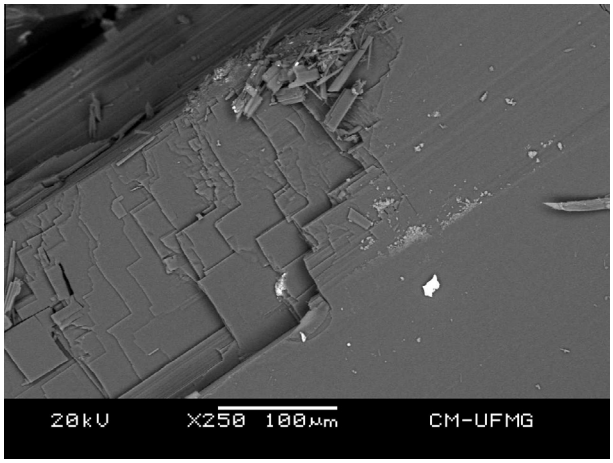

Fig. 2. BSI image of meyerhofferite.

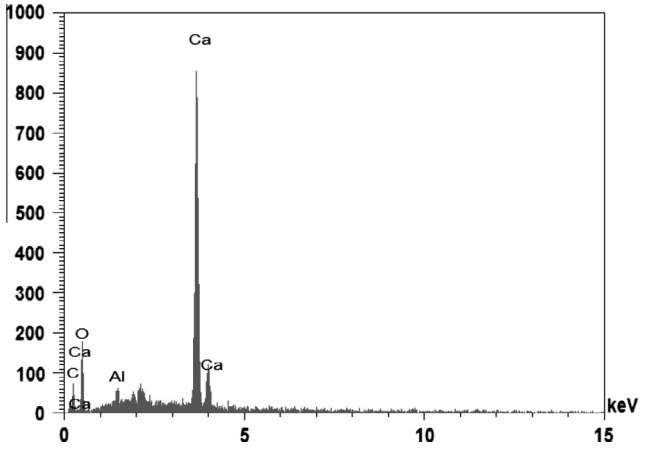

Fig. 3. EDS analysis of meyerhofferite.

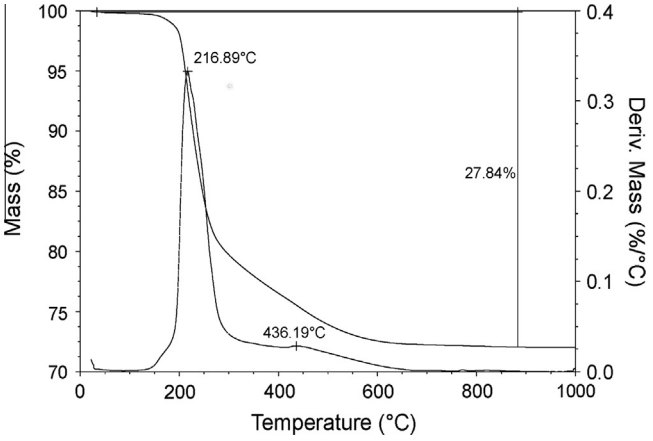

Fig. 4. TG/DTG graphic.

The quantitative chemical analysis of meyerhofferite is presented in Table 1. The composition was calculated as mean values in three spots. The range of the chemical analysis is also presented, and shows no significant variance. H_2O content was calculated by thermogravimetric analysis and B_2O_3 was calculated by stoichiometry. The chemical formula was calculated on the basis of 9 oxygen

Table 1
Chemical composition of meyerhofferite (mean of 3 spots). H_2O calculated by thermogravimetric analysis and B_2O_5 calculated by stoichiometry.

Constituent	wt.%	Range (wt.%)	Number of atoms	Probe standard
CaO	22.01	21.75–22.38	0.97	Anorthite100
B_2O_3	46.71		3.09	Calculated by stoichiometry
MgO	0.00	0.00–0.01	0.00	MgO
Al_2O_3	0.00	0.00–0.00	0.00	Anorthite100
P_2O_5	0.02	0.00–0.05	0.00	$Ca_2P_2O_7$
As_2O_5	0.04	0.00–0.08	0.00	Arsenopyrite
ZnO	0.01	0.00–0.03	0.00	Sphalerite
MnO	0.01	0.00–0.03	0.00	Rodhonite
FeO	0.00	0.00	0.00	Magnetite
SiO_2	0.00	0.00	0.00	Anorthite100
F	0.00	0.00	0.00	Fluorite
H_2O	27.84	H_2O	0.97	Calculated by thermogravimetric analysis
		OH	4.87	
Total	96.64		9.90	

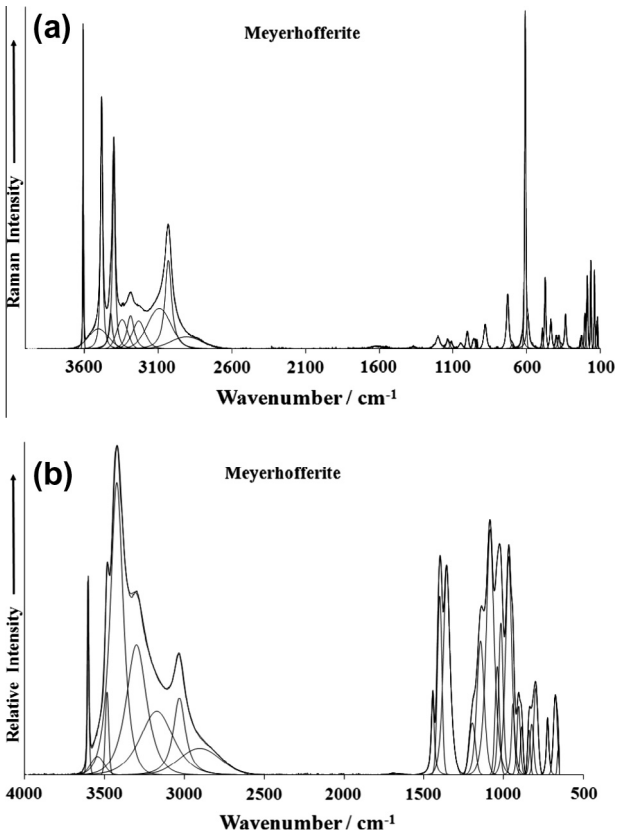

Fig. 5. (a) Raman spectrum of meyerhofferite in the 100–4000 cm^{-1} region, (b) infrared spectrum of meyerhofferite in the 500–4000 cm^{-1} region.

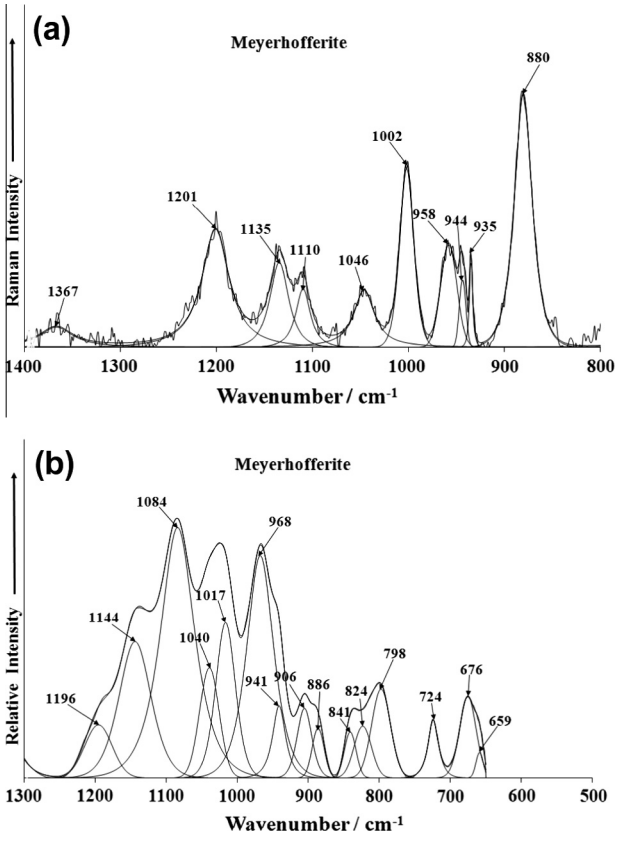

Fig. 6. (a) Raman spectrum of meyerhofferite (upper spectrum) in the 800–1400 cm^{-1} spectral range and (b) infrared spectrum of meyerhofferite (lower spectrum) in the 500–1300 cm^{-1} spectral range.

atoms in the structure. The chemical composition indicates a pure phase with minor amounts of As, P, Mn and Zn. The chemical formula of the studied sample can be expressed as: $Ca_{0.97}(B_{3.09}O_3)(OH)_{4.87}{\cdot}0.97(H_2O)$.

Vibrational spectroscopy

The Raman spectrum of meyerhofferite over the 100–4000 cm^{-1} spectral range is displayed in Fig. 5a. This spectrum reports the position and relative intensity of the individual Raman bands. The most intense band is located in the OH stretching region. In the spectrum, there are obvious spectral regions in which no intensity is observed. Thus, the spectral analysis is divided into sections depending upon the type of vibrations being observed. The infrared spectrum over the 500–4000 cm^{-1} spectral range is shown in Fig. 5b. Compared with the Raman spectrum, much greater intensity is found in the infrared spectrum. As with the Raman spectrum, the infrared spectrum is subdivided into sections for more detailed analysis, depending on the type of vibration being observed.

The Raman spectrum in the 800–1400 cm^{-1} spectral region is displayed in Fig. 6a. In comparison, the infrared spectrum in the 500–1300 cm^{-1} region is shown in Fig. 6b. This spectral region is where the trigonal and tetrahedral borate bands are observed. A very intense Raman band is observed at 880 cm^{-1}. This band is assigned to the symmetric stretching mode of trigonal borate. The symmetric stretching mode of tetrahedral boron is normally observed in the 700–850 cm^{-1} spectral region. The intense Raman band at 609 together with the Raman band at 728 cm^{-1} are assigned to this vibrational mode (Fig. 7a). The four bands at 935, 944, 958 and 1002 cm^{-1} are attributed to the antisymmetric

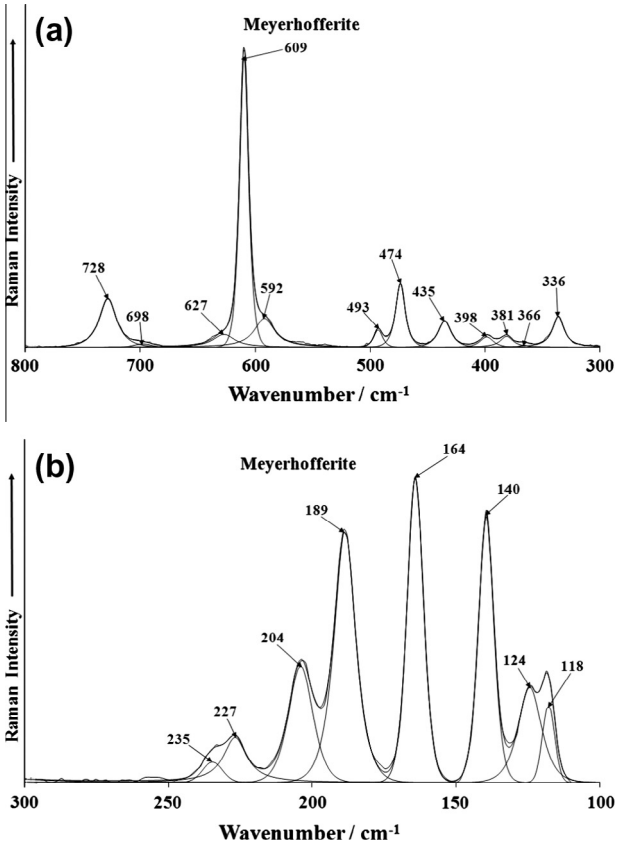

Fig. 7. (a) Raman spectrum of meyerhofferite (upper spectrum) in the 300–800 cm^{-1} spectral range and (b) Raman spectrum of meyerhofferite (lower spectrum) in the 100–300 cm^{-1} spectral range.

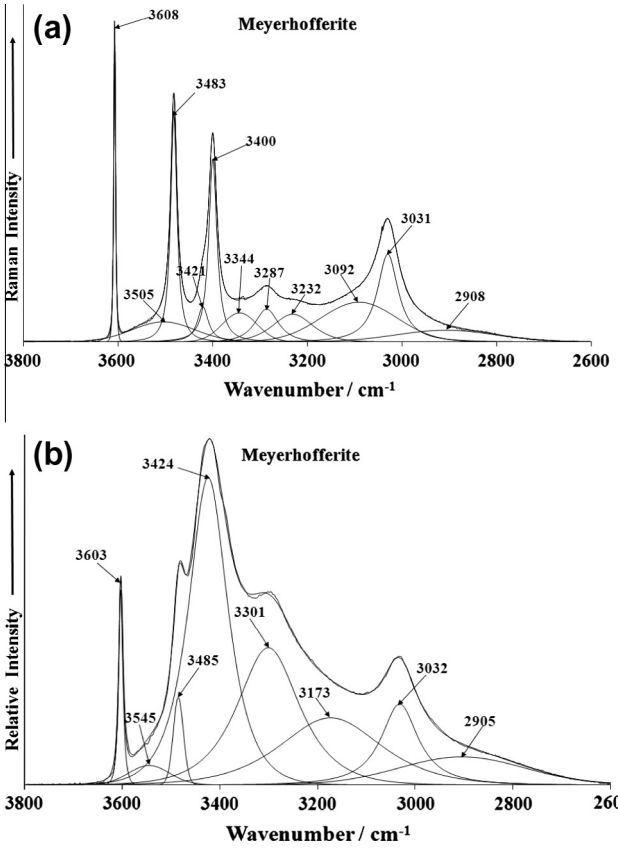

Fig. 8. (a) Raman spectrum of meyerhofferite (upper spectrum) in the 2600–4000 cm^{-1} spectral range and (b) infrared spectrum of meyerhofferite (lower spectrum) in the 2600–4000 cm^{-1} spectral range.

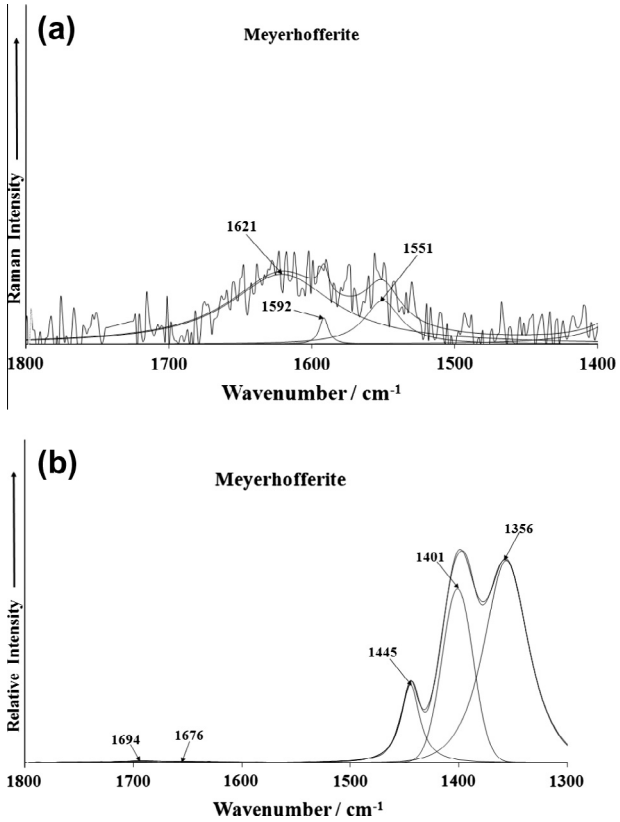

Fig. 9. (a) Raman spectrum of meyerhofferite (upper spectrum) in the 1400–2000 cm^{-1} spectral range and (b) infrared spectrum of meyerhofferite (lower spectrum) in the 1300–1800 cm^{-1} spectral range.

stretching vibrations of tetrahedral boron. The Raman bands at 1110, 1135, 1201 cm^{-1} are attributed to the BOH in-plane bending modes. According to Ross [30] (page 220 of this reference), bands between 1300 and 1500 cm^{-1} are due to the antisymmetric stretching modes of trigonal boron. The broad band at 1367 cm^{-1} may therefore be assigned to the stretching vibration of trigonal boron.

The infrared spectrum of meyerhofferite shows complexity with a series of overlapping bands. Ross [30] (page 222 of this reference) reported the infrared spectrum of meyerhofferite and drew attention to the infrared spectrum of the borate mineral inyoite. The infrared spectra of several borate minerals [29,34] have been determined but no band assignments were made. The infrared spectra of some synthetic borates has been compared with the infrared spectra of some selected natural borates [35]. No band assignment was undertaken. The infrared bands are more likely to reflect the antisymmetric stretching vibrations as opposed to the symmetric stretching vibrations which are more intense in the Raman spectrum. Thus, the infrared band at 968 cm^{-1} is assigned to the asymmetric stretching vibration of tetrahedral boron. The strong infrared bands at 1084, 1144 and 1196 cm^{-1} are due to the OH in-plane bending modes. The series of infrared bands in the 800–900 cm^{-1} spectral range are best described as the symmetric stretching of tetrahedral boron. The infrared bands at 659, 676 and 724 cm^{-1} are assigned to the bending modes of trigonal and tetrahedral boron. These bands are observed as low intensity bands in the Raman spectrum and are observed at 627, 698 and 728 cm^{-1} (Fig. 7a). A series of low intensity Raman bands are observed at 366, 381, 398. A series of low intensity Raman bands are observed at 366, 381, 398, 435, 474 and 493 cm^{-1}. It is probable that these bands could also be assigned to borate bending modes. The bands in the 100–300 cm^{-1} spectral region (Fig. 7b) are assigned to lattice vibrations.

The Raman and infrared spectra of meyerhofferite mineral in the 2600–3800 cm^{-1} spectral range are displayed in Fig. 8a and b. Meyerhofferite contains both water and hydroxyl units, and therefore bands would be expected from these moieties. The very sharp Raman bands at 3400, 3483 and 3608 cm^{-1} and the equivalent infrared bands at 3485 and 3603 cm^{-1} are assigned to the stretching vibration of the hydroxyl units. The Raman bands at 3031, 3092, 3232, 3287 and 3344 cm^{-1} are attributed to water stretching bands. Such bands show much greater intensity in the infrared spectrum; bands are observed at 3032, 3173, 3301 and 3424 cm^{-1}. The Raman spectrum in the 1400–1800 cm^{-1} spectral region is provided in Fig. 9a. The spectrum suffers from a lack of signal; nevertheless a broad band is identified at 1621 cm^{-1} and is assigned to the bending mode of water. This band is identified as the bands at 1676 and 1694 cm^{-1} in the infrared spectrum. The position of these bands is indicative of strongly hydrogen bonded water. Intense infrared bands are found at 1356, 1401 and 1445 cm^{-1}. These bands are assigned to the antisymmetric stretching of trigonal boron.

Conclusions

There are many borate minerals which have yet to have their vibrational spectrum determined and the molecular structure assessed in terms of their vibrational spectrum. Included in this group of natural borates is the mineral meyerhofferite, which to the best of the authors' knowledge has not had its Raman spectrum analyzed. In this work we have measured the Raman and infrared spectrum of meyerhofferite over the complete spectral range.

The combined chemical characterization via SEM, EDS and TG shows a pure phase with limited cationic substitution. The chemical formula can be expressed as $Ca_{0.97}(B_{3.09}O_3)(OH)_{4.87}{\cdot}0.97(H_2O)$.

The infrared spectrum of meyerhofferite is complex with overlapping bands, making the assignment of the infrared bands difficult. Further, the infrared technique has a spatial resolution of at best 25 μm. The Raman spectrum of meyerhofferite results in a clearly resolved sets of bands and because the spatial resolution is around 1 μm, individual crystals of meyerhofferite may be analyzed by Raman spectroscopy. The two techniques of Raman and infrared spectroscopy are complimentary. For example in the OH stretching region, Raman spectroscopy more readily determines the stretching vibrations of the OH units, whereas infrared spectroscopy detects water more readily.

One of the difficulties in analyzing the spectra of meyerhofferite is to state which bands are due to trigonal and tetrahedral boron. The Raman spectrum of meyerhofferite is dominated by intense sharp band at 880 cm^{-1} assigned to the symmetric stretching mode of trigonal boron. Broad Raman bands at 1046, 1110, 1135 and 1201 cm^{-1} are attributed to BOH in-plane bending modes. Raman bands in the 900–1000 cm^{-1} spectral region are assigned to the antisymmetric stretching of tetrahedral boron. Both the Raman and infrared spectrum of meyerhofferite in the hydroxyl stretching region show intense bands. In the Raman spectrum, the intensity of the bands attributed to the hydroxyl units are far more intense than the bands assigned to water stretching vibrations. This is because water is such a poor Raman scatterer. On the other hand water is such a very intense absorber; the infrared bands are very strong whereas the infrared bands of the OH units are significantly lower. Distinct OH stretching Raman bands are observed at 3400, 3483 and 3608 cm^{-1}. The mineral meyerhofferite has a distinct Raman spectrum which is different from the spectrum of other borate minerals, making Raman spectroscopy a very useful tool for the detection of meyerhofferite.

Acknowledgments

The financial and infra-structure support of the Queensland University of Technology, Chemistry discipline is gratefully acknowledged. The Australian Research Council (ARC) is thanked for funding the instrumentation. The authors would like to acknowledge the Center of Microscopy at the Universidade Federal de Minas Gerais (http://www.microscopia.ufmg.br) for providing the equipment and technical support for experiments involving electron microscopy. R. Scholz thanks to CNPq – Conselho Nacional de Desenvolvimento Científico e Tecnológico (Grant No. 306287/2012-9).

Appendix A. Supplementary material

Supplementary data associated with this article can be found, in the online version, at http://dx.doi.org/10.1016/j.saa.2013.05.016.

References

[1] W.T. Schallier, U.S. Geol, Survey Bull. 610 (1916) 35–55.
[2] W.F. Foshag, Am. Mineral. 9 (1924) 8–10.
[3] J.W. Anthony, R.A. Bideaux, K.W. Bladh, M.C. Nichols, Handbook of Mineralogy, Borates, Carbonates, Sulfates, vol. 5, Mineral Data Publishing, Tucson, Arizona, 1990.
[4] R. Birsoy, U. Oezbas, Carbon. Evap. 27 (2012) 71–85.
[5] C.L. Christ, J.R. Clark, Acta Cryst. 9 (1956) 830.
[6] C.L. Christ, J.R. Clark, Zeit. Fuer Kristall. 114 (1960) 321–342.
[7] J.R. Clark, C.L. Christ, Zeit. Fuer Kristall. 112 (1959) 213–233.
[8] C. Palache, Am. Mineral. 23 (1938) 644–648.
[9] P.C. Burns, F.C. Hawthorne, Can. Mineral. 31 (1993) 305–312.
[10] R. Birsoy, Turk Muhend. ve Cevre Bilim. Derg. 12 (1988) 188–194.
[11] J.B. Farmer, A.J.D. Gilbert, P.J. Haines, in: Proc. 7th Int. Conf. Therm. Anal., vol. 1, 1982, pp. 650–656.
[12] I. Ardelean, S. Cora, J. Mater. Sc. 19 (2008) 584–588.
[13] I. Ardelean, S. Cora, J. Optoelectron Adv. Mater. 12 (2010) 239–243.
[14] I. Ardelean, L. Griguta, J. Optoelectron. Adv. Mater. 9 (2007) 2068–2070.
[15] I. Ardelean, V. Timar, J. Optoelectron Adv. Mater. 10 (2008) 246–250.
[16] F.H. El Batal, M.A. Azooz, A.A. El-Kheshen, Trans. Ind. Ceram. Soc. 68 (2009) 81–90.
[17] F.H. ElBatal, Y.M. Hamdy, Trans. Ind. Ceram. Soc. 67 (2008) 193–202.
[18] C. Rajyasree, P.M. Vinaya Teja, K.V.R. Murthy, D. Krishna Rao, Condense. Mater. 406 (2011) 4366–4372.
[19] B. Sumalatha, I. Omkaram, T.R. Rao, C.L. Raju, J. Non-Cryst. Solids 357 (2011) 3143–3152.
[20] M. Mir, J. Janczak, Y.P. Mascarenhas, J. Appl. Cryst. 39 (2006) 42–45.
[21] I. Mitov, Z. Cherkezova-Zheleva, V. Mitrov, J. Balkan Trib. Ass. 4 (1998) 191–200.
[22] A.S. Povarennykh, E.I. Nefedov, Geol. Zh. 31 (1971) 13–27.
[23] V.S. Suknev, E.N. Diman, Zh. Prikladnoi Spektros. 10 (1969) 326–328.
[24] V.F. Ross, J.O. Edwards, Chem. Boron Its Compd. (1967) 15–207.
[25] R.L. Frost, J. Raman Spectrosc. 42 (2011) 540–543.
[26] M.V. Akhmanova, Zh. Struk. Khim. 3 (1962) 28–34.
[27] D.A. Long, R.T. Bailey, Spectrochim. Acta 19 (1963) 1607–1610.
[28] A. Vasko, I. Srb, Czech. J. Phys. 17 (1967) 1110–1123.
[29] C.E. Weir, Phys. Chem. 70 (1966) 153–164.
[30] V.C. Farmer, Mineralogical Society Monograph 4: The Infrared Spectra of Minerals, London, 1974.
[31] C. Helvaci, Mercian Geol. 6 (1978) 257–270.
[32] C. Helvaci, R.N. Alonso, Turk. J. Earth Sci. 9 (2000) 1–27.
[33] C. Helvaci, R.J. Firman, Trans. Inst. Min. Metall. 85 (1976) 142–152.
[34] E.V. Vlasova, M.G. Valyashko, Zh. Neor. Khim. 11 (1966) 1539–1547.
[35] M.G. Valyashko, E.V. Vlasova, Jena Rev. 14 (1969) 3–11.